



CDF note 7161

Search for MSSM Higgs Decaying to Tau Pairs

The CDF Collaboration
URL <http://www-cdf.fnal.gov>
(Dated: July 31, 2004)

We present the results of a search for a neutral MSSM Higgs boson decaying to a pair of tau leptons. The analyzed data sample corresponds to integrated luminosity of approximately 200 pb^{-1} of $p\bar{p}$ collisions at $\sqrt{s} = 1.96 \text{ TeV}$. It was collected by the CDF detector during Run 2 of the Fermilab Tevatron. We select tau pairs in which one of the taus decays hadronically and the other to e or μ and neutrinos. We see no evidence of signal and perform a fit to the (partially) reconstructed di-tau mass to set limits on the product of Higgs production cross-section and its branching fraction to taus.

Preliminary Results for Summer 2004 Conferences

I. INTRODUCTION

The Minimal Supersymmetric Standard Model (MSSM) predicts the existence of three neutral and two charged Higgs bosons. At hadronic colliders, the production cross section of the pseudoscalar neutral boson A scales as $\tan^2 \beta$, where $\tan \beta$ is one of the parameters of the theory. The major decay modes of A are $A \rightarrow b\bar{b}$ ($\sim 90\%$), and $A \rightarrow \tau\tau$ ($\sim 8\%$). While the branching fraction to $b\bar{b}$ is much larger and $b\bar{b} \rightarrow Ab\bar{b}$, $A \rightarrow b\bar{b}$ is considered the most promising channels at the Tevatron, the important production mechanisms $gg \rightarrow A$, $b\bar{b} \rightarrow A$ are difficult to study in the $A \rightarrow b\bar{b}$ channel due to large backgrounds. The addition of the $A \rightarrow \tau\tau$ mode expands our reach and is an important part of the MSSM Higgs search effort at CDF.

Detailed information on Higgs production at the Tevatron and detection possibilities by the CDF and D0 experiments can be found in [1].

II. DATA SAMPLE & EVENT SELECTION

Our signal consists of a tau pair in which one of the taus decays to hadrons and a neutrino (τ_h) while the other decays to an electron or muon and two neutrinos (τ_e or τ_μ).

This analysis is based on an integrated luminosity of approximately 200 pb^{-1} collected with the CDF detector [2] between March 2002 and January 2004. The data are collected with a set of dedicated τ -triggers incorporated in the trigger system for Run 2. These triggers select a lepton (e, μ) candidate and an isolated track. The e +track trigger requires an “electron” track $p_T > 8 \text{ GeV}$ matched to an EM calorimeter tower with $E_T^{EM} > 8 \text{ GeV}$, and a “pion” track with $p_T > 5 \text{ GeV}$ separated from the electron candidate by at least 10 degrees in the azimuthal plane. Since hadronic tau decays at high energies appear as narrow jets, the trigger also requires the “pion” track to be isolated with no other charged tracks in an annulus between 0.17 and 0.52 radians around it. The μ +track trigger requires a track with $p_T > 8 \text{ GeV}$ with associated hits in the muon chambers. The “pion” track requirements are the same as those described above for the electron+track.

A. Tau Reconstruction and Isolation

Our initial data sample is dominated by di- and multi-jet events, and leptonic decays of W and Z bosons.

Backgrounds from $jet \rightarrow tau$ misidentification are suppressed by applying stricter isolation requirements on the τ_h candidate.

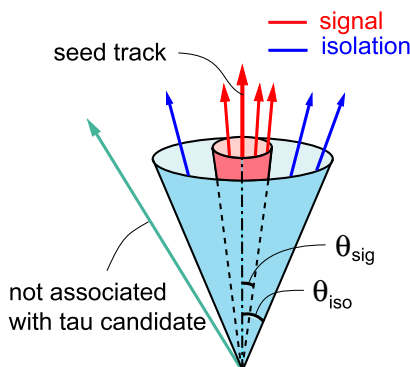


FIG. 1: Tau signal cone and isolation annulus for tracks and π^0 's. The inner cone contains the τ_h .

Tau reconstruction starts with finding a seed calorimeter tower with transverse energy $E_T^{seed \text{ } twr} > 6 \text{ GeV}$. Adjacent shoulder towers with energies $E_T^{sh \text{ } twr} > 1 \text{ GeV}$ are added to form a calorimeter cluster. The number of towers in the cluster must be less than or equal to six.

The next step is to associate tracks with the tau candidate. A track with $p_T > 6$ GeV/c pointing to the calorimeter cluster is chosen as the “seed track” and neighboring tracks with $p_T > 1$ GeV/c are added to the tau candidate. The signal cone and isolation annulus are defined with respect to the seed track as shown in Figure 1. The angle θ_{sig} is the minimum of 0.17 rad or $5.0 / E^{\tau \text{ cl}}$ (in GeV). The isolation annulus goes out to $\theta_{\text{iso}} = 0.52$ rad. Tracks within angle θ_{sig} of the seed track are considered tau decay products, while ones with $\theta_{\text{sig}} < \theta < \theta_{\text{iso}}$ are treated as isolation tracks and used to veto tau candidates.

Hadronic tau decays often include neutral pions. They are reconstructed using position information from the CES detector and energy deposition in the EM calorimeter. Neutral pions are associated with the tau candidate using the same criteria as applied for charged tracks. We require the invariant mass of the tracks and π^0 's of the tau candidate to be less than $1.8 \text{ GeV}/c^2$.

We suppress electrons misidentified as pions by requiring the ratio of the energy deposited in the hadronic calorimeter to the sum of charged tracks' momenta to be greater than 0.2. Note that we cannot use energy deposited in the electromagnetic calorimeter as the basis of an electron veto due to the presence of π^0 's in tau decays.

B. Event Cuts

The sample of tau candidates selected with the criteria outlined in the previous section has significant contamination from quark and gluon jets. We define the scalar sum

$$\hat{H}_T = |p_T^{\text{vis}}(\tau_1)| + |p_T^{\text{vis}}(\tau_2)| + \cancel{E}_T,$$

where $p_T^{\text{vis}}(\tau)$ is the transverse momentum of the tau decay products not including neutrinos, and \cancel{E}_T is the missing transverse energy and use it to suppress these backgrounds. Figure 2 shows the distribution of \hat{H}_T for a jet dominated sample, $Z \rightarrow \tau\tau$ and Higgs signal. Requiring \hat{H}_T to be greater than 50 GeV leads to significant background reduction with small signal loss.

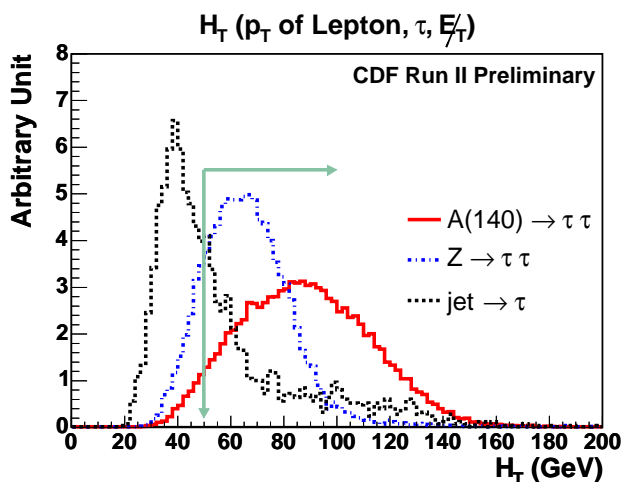


FIG. 2: Distribution of \hat{H}_T for Z , Higgs (A of mass $140 \text{ GeV}/c^2$), and a jet-dominated data sample. All distributions are normalized to unit area. The line shows the cut at 50 GeV.

We require events to be consistent with the signature expected from a particle decaying to two taus. Assuming that \cancel{E}_T in the event is due to the neutrinos from tau decays, it should not point in direction opposite to the tau decay products. Since only the transverse component of missing energy is measured, this requirement is restricted to the transverse plane. We define a unit vector along the bisection axis of the visible tau decay products ($\hat{\zeta}$) as shown in Figure 3, and two projection variables, p_{ζ}^{vis} and p_{ζ} .

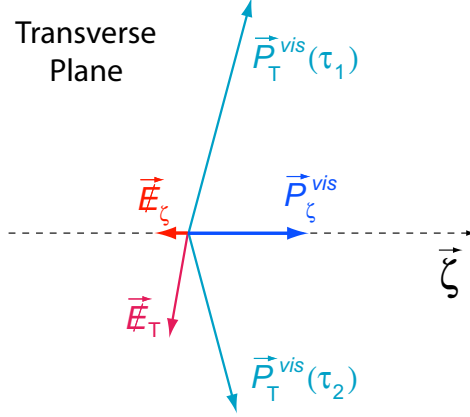


FIG. 3: Illustration of the definition of parameters used in the ζ cut.

The first is the sum of the projection of both visible tau p_T onto the bisection vector ($p_\zeta^{vis} = \vec{p}_{\tau_1}^{vis} \cdot \hat{\zeta} + \vec{p}_{\tau_2}^{vis} \cdot \hat{\zeta}$). The second is the sum of p_ζ^{vis} and the projection of the \vec{E}_T onto the bisection vector ($p_\zeta = p_\zeta^{vis} + \vec{E}_T \cdot \hat{\zeta}$). Figure 4 shows the separation between signal and W plus jet(s) background in the p_ζ^{vis} , p_ζ plane.

The electron candidate is required to have $E_T > 10$ GeV and $p_T > 8$ GeV/c. The ratio of the hadronic calorimeter to electromagnetic calorimeter deposit has to be less than $0.055 + 0.00045 \times E$. Additional requirements on E/p , calorimeter isolation, CES energy deposit, and track quality improve the purity of the electron sample.

The muons are required to have $p_T > 10$ GeV/c, and matched to a stub in the appropriate muon detectors. The energy deposited in the calorimeter is required to be small, consistent with a minimum ionizing track plus accidental activity.

Events consistent with $Z \rightarrow e^+e^-$ and $Z \rightarrow \mu^+\mu^-$ are suppressed by requiring that the invariant mass calculated using an e^+e^- or $\mu^+\mu^-$ assumption be outside a 25 GeV/ c^2 window of the Z boson mass.

Finally, we require the tau candidate to have either one or three tracks, and opposite charge from the e or μ .

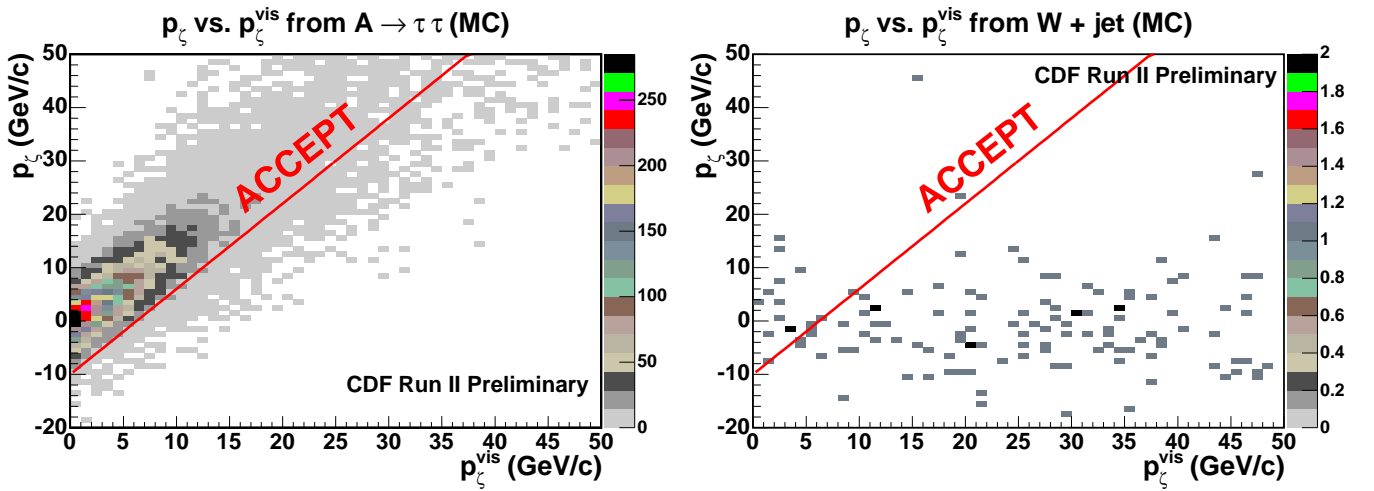


FIG. 4: Effect of the ζ cut on Higgs signal (A of mass 140 GeV/ c^2 , left) and $W + \text{jet}(s)$ MC events (right).

III. SIGNAL ACCEPTANCE AND BACKGROUND ESTIMATION

We used the Pythia MC generator, version 6.216 [3] to simulate the processes $gg \rightarrow A$ and $\bar{b}b \rightarrow A$. The Higgs boson was forced to decay to $\tau^+\tau^-$. The taus are decayed using the Tauola package [4]. We generated Higgs masses between $115 \text{ GeV}/c^2$ and $200 \text{ GeV}/c^2$ for $\tan\beta = 30$. Figure 5 shows the *total* efficiency for detecting a Higgs decaying to specific tau final states. The relevant τ branching fractions are included in the acceptance.

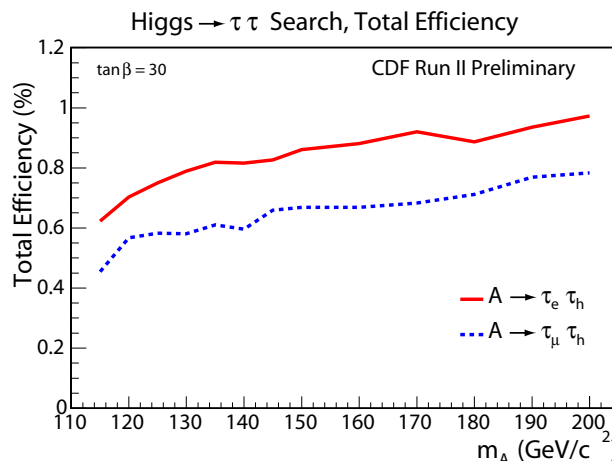


FIG. 5: Detection efficiency as a function of Higgs mass. The efficiencies were calculated with Monte Carlo sets generated with $\tan\beta = 30$.

The biggest source of background are $Z \rightarrow \tau\tau$ events which can only be distinguished from the Higgs signal by the ditau parent mass. However, the presence of multiple neutrinos in the final state makes full reconstruction of the parent mass impossible in the general case. We estimate $Z \rightarrow e^+e^-$, $Z \rightarrow \mu^+\mu^-$, di-boson and $t\bar{t}$ events by using Monte Carlo samples. Backgrounds from $jet \rightarrow \tau$ misidentification are estimated using a fake rate function obtained from independent jet samples. The fake rate is parameterized in terms of jet energy, pseudorapidity (η) and track multiplicity.

Figure 6 (left) shows the track multiplicity for hadronically decaying tau candidates. The enhancement at one and three tracks is a characteristic signature of tau decays. For this plot, all selection criteria except the track multiplicity and opposite charge requirement have been applied. The figure also shows the invariant mass of the tracks and π^0 's (right), after applying the full set of cuts.

Predicted backgrounds and observed number of events after applying all cuts are listed in Table I.

	$\tau_h\tau_e$	$\tau_h\tau_\mu$	Combined
$Z \rightarrow \tau\tau$	132.3 ± 17.1	104.1 ± 13.3	236.4 ± 29.5
$Z \rightarrow ll$	1.8 ± 0.2	4.9 ± 0.4	6.7 ± 0.6
$t\bar{t}, VV$	0.7 ± 0.1	0.8 ± 0.1	1.5 ± 0.1
$jet \rightarrow \tau$	12.0 ± 3.6	7.0 ± 2.1	19.0 ± 5.7
Total predicted	146.8 ± 17.5	116.8 ± 13.5	263.6 ± 30.1
Data	133	103	236

TABLE I: Predicted backgrounds and observed events after applying all selection criteria.

Table II summarizes the systematic uncertainties used in the analysis. PDF's refer to the uncertainty due to the Parton Distribution Function in the proton. CMUP and CMX refer to two different muon triggers.

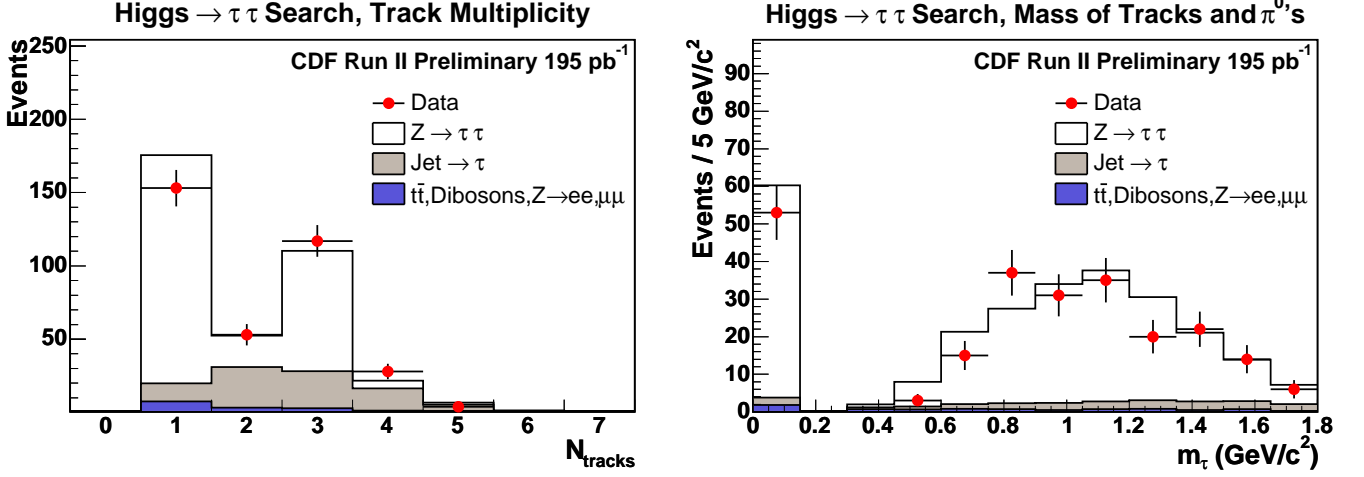


FIG. 6: Track multiplicity (left) and invariant mass of tracks and π^0 's (right) for the tau candidates. Track multiplicity and opposite charge cuts are not applied on the left plot.

Parameter	Sys error(%)
e ID	4
μ ID	4
τ ID	10
Event cuts (\hat{H}_T, ζ)	1
$jet \rightarrow \tau$ fakes	30
$\sigma \times \mathcal{B}(Z \rightarrow ll)$	2.1
PDFs (Z, W)	3
PDFs ($Higgs$)	7.5
Luminosity	6
$e + track$ trig	2
$\mu(CMUP) + track$ trig	2
$\mu(CMX) + track$ trig	2

TABLE II: Systematic uncertainties used in the analysis. The uncertainty in $jet \rightarrow \tau$ misidentification is large, but applies to a small value.

IV. RESULTS

Since $Z \rightarrow \tau\tau$ decays differ from our Higgs signal only in mass, we define a mass-like discriminating variable $m_{vis}(\ell, \tau_h^{vis}, \cancel{E}_T)$. It is constructed using the four-momentum of the lepton ($\ell = e$ or μ), the four-momentum of the visible decay products of the τ_h (τ_h^{vis}) and \cancel{E}_T (also treated as a four-vector). Figure 7 shows the discriminating power of m_{vis} . Due to the partial mass reconstruction the distributions are not centered at the true masses.

After combining the $\tau_e\tau_h$ and $\tau_\mu\tau_h$ channels we perform a binned likelihood fit of the $m(\ell, \tau_h^{vis}, \cancel{E}_T)$ distribution to extract a Higgs signal. The uncertainties in background estimation are incorporated in the imposed Gaussian constraints. Several signal templates were generated to cover the studied mass region. Figure 8 shows the $m_{vis}(\ell, \tau_h^{vis}, \cancel{E}_T)$ distribution for data and various backgrounds. The limits on Higgs production cross-section times branching fraction at 95% CL are presented in Figure 9. Presently, we are only sensitive to Higgs production at large $\tan\beta$.

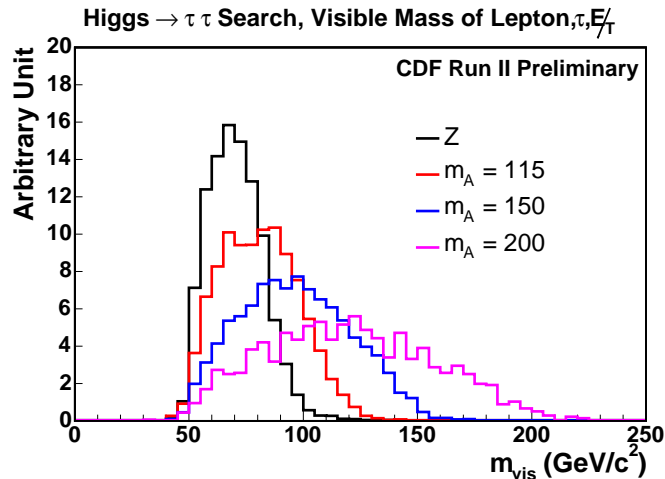


FIG. 7: Distributions of $m_{vis}(\ell, \tau_h^{vis}, \cancel{E}_T)$ for Z and Higgs at several mass points.

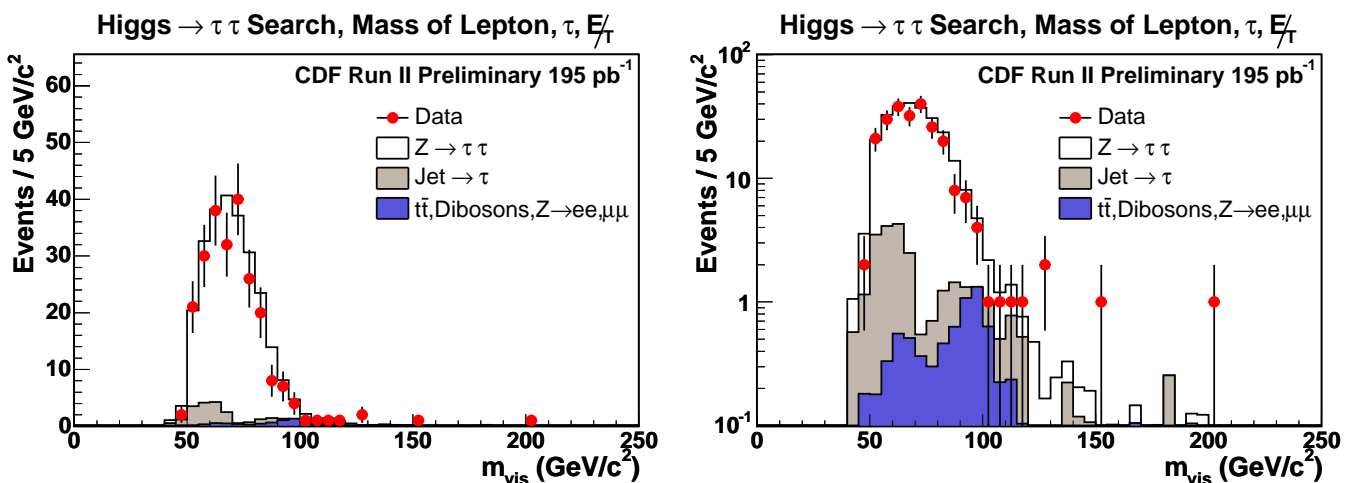


FIG. 8: Observed $m(\ell, \tau_h^{vis}, \cancel{E}_T)$ distribution and predictions for various backgrounds. The left and right plots show the same data, but in a linear and logarithmic scales.

V. CONCLUSION

We have performed a search for a neutral MSSM Higgs decaying to tau pairs, and set limits on production cross section times branching ratio. We are planning to increase the sensitivity of our search through addition of more data and inclusion of the $\tau_e\tau_\mu$ and $\tau_h\tau_h$ channels.

Acknowledgments

We thank the Fermilab staff and the technical staffs of the participating institutions for their vital contributions. This work was supported by the U.S. Department of Energy and National Science Foundation; the Italian Istituto Nazionale di Fisica Nucleare; the Ministry of Education, Culture, Sports, Science and Technology of Japan; the Natural Sciences and Engineering Research Council of Canada; the National Science Council of the Republic of

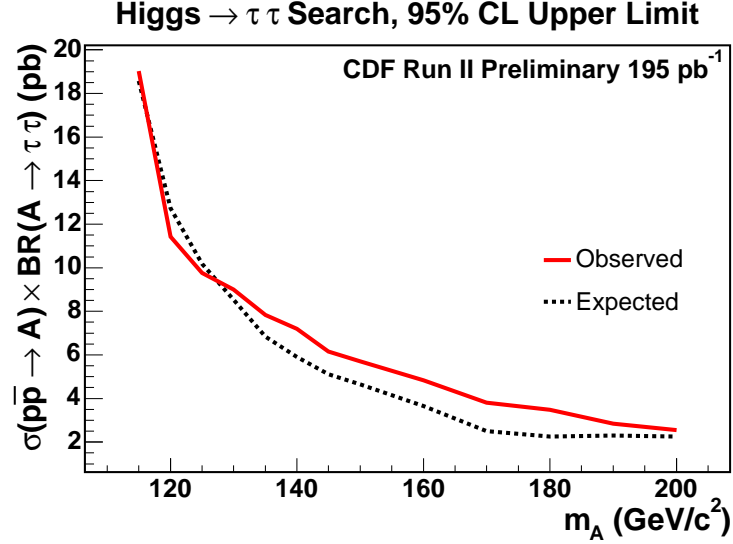


FIG. 9: *Observed (solid) and expected from psuedoexperiments (dashed) limits on the product $\sigma(p\bar{p} \rightarrow A) \times \text{BR}(A \rightarrow \tau\tau)$.*

China; the Swiss National Science Foundation; the A.P. Sloan Foundation; the Bundesministerium fuer Bildung und Forschung, Germany; the Korean Science and Engineering Foundation and the Korean Research Foundation; the Particle Physics and Astronomy Research Council and the Royal Society, UK; the Russian Foundation for Basic Research; the Comision Interministerial de Ciencia y Tecnologia, Spain; and in part by the European Community's Human Potential Programme under contract HPRN-CT-20002, Probe for New Physics.

-
- [1] Report of the Tevatron Run 2 Higgs Working Group, eprint archive: hep-ph/0010338.
 - [2] F. Abe, et al., Nucl. Instrum. Methods Phys. Res. A **271**, 387 (1988); D. Amidei, et al., Nucl. Instrum. Methods Phys. Res. A **350**, 73 (1994); F. Abe, et al., Phys. Rev. D **52**, 4784 (1995); P. Azzi, et al., Nucl. Instrum. Methods Phys. Res. A **360**, 137 (1995); The CDFII Detector Technical Design Report, Fermilab-Pub-96/390-E
 - [3] T. Sjostrand et al., High-Energy-Physics Event Generation with PYTHIA 6.1, Comput. Phys. Commun. **135**, 238 (2001).
 - [4] Jadach, Z. Was and J.H. Kuehn, TAUOLA — A library of Monte Carlo programs to simulate decays of polarized leptons, Comp. Phys. Commun. **64** (1991).